This is a post-peer-review, pre-copyedit version of an article published in [Journal of the Brazilian Society of Mechanical Sciences and Engineering]. The final authenticated version is available online at: [https://doi.org/10.1007/s40430-024-05141-0]".

Investigation of rock porosity using vibroacoustography

João H. Uliana[a], Guilherme A. Braz[a], Éverton L. Oliveira[b], Arthur G. Araújo-Ferreira[b], Mateus M. Morais[c], Willian A. Trevizan[d], Carlos A. Fortulan[c], Tito J. Bonagamba[b], Theo Z. Pavan[a], Antonio A. O. Carneiro[a]

[a]*Department of Physics, FFCLRP, University of São Paulo, Ribeirão Preto, Brazil*

[b]*São Carlos Institute of Physics, University of São Paulo, São Carlos, Brazil*

[c]*São Carlos School of Engineering, University of São Paulo, São Carlos, Brazil*

[d]*Cenpes, Petrobras Research Center, Rio de Janeiro, Brazil*

Abstract

The porosity of materials influences several physical parameters, such as resistance to fractures, thermal conductivity, and fluid flow permeability. The quantification of porosity is important in various fields, ranging from industry to biomedicine. Although various techniques are available to quantify porosity in laboratory environments, its analysis applied in the context of nondestructive tests in industry or biomedical protocols can be challenging. To contribute to the development of alternative methods for measuring the porosity of a material, this paper investigated the feasibility of using vibroacoustography, a low-cost, nondestructive, and noncontact technique, to estimate the porosity of rock samples. The study examined the vibroacoustic response as a function of porosity in synthetic ceramic samples produced using the same material with controlled porosity percentages. Then, the vibroacoustography technique was applied to a realistic case of sandstone rocks with varying porosities. The results showed that the new protocol can be used to estimate the porosity as it demonstrates a relationship between the amplitude of vibroacoustic signals and the porosity of rock samples. These findings could be valuable in exploring and characterizing oil reservoir rocks. **Keywords:** *Porous media, Porosity, Vibroacoustography, Nondestructive Test, Ultrasound, Image, Nuclear magnetic resonance.*

1. Introduction

Porosity is an important physical parameter that attracts interest in several areas, including industry and biomedicine. In industry, the porosity of materials is related to the physical interactions and chemical reactivity of many industrial processes [1], and it can also impact the permeability of rocks to the flow of oil in reservoirs [2]. Additionally, porous materials are interesting for the production of building materials due to their thermal conductivity [3]. In biomedicine, porosity is related to bone health, resistance to fractures, and the development of biocompatible scaffolds for bone tissue regeneration [4]–[7].

Porosity is the void fraction within a material [3]. Although it is simple to define, it is challenging to quantify and qualify due to the complex and varied morphology and interrelationship of pores, which can have dimensions ranging from a few nanometers to centimeters. Several imaging methods have been applied to measure pore size distribution, porosity, and microstructure characterization [3]. For example, optical microscopy, scanning electron microscopy, and X-ray computed tomography are popular nondestructive analysis methods for porous media that provide information about microstructure and quantify porosity [8]. Ultrasound transmission techniques are also used to quantify porosity in materials and analyze petrophysical properties using several modalities, including ultrasound transmission, measurements with different incident angles, analysis of wave phase, and measurements of velocity and attenuation based on the classical Biot theory [9]–[14]. Nuclear magnetic resonance (NMR) is another technique used for the characterization of porous media. The NMR signal from fluid molecules within pores provides estimates of porosity, permeability, and pore size distribution [15], [16].

While the aforementioned methods are well-suited for laboratory analysis, their complexity, cost, or geometry may pose challenges to their application in nondestructive tests (NDT) in industrial processes or biomedical protocols. Methods that rely on the transmission of ultrasound waves or X-ray photons may be affected by the sample size due to the path length in the porous media and the need for a detector on the opposite side [17], [18]. Additionally, super-resolution microscopy techniques, which use high-resolution detection of electrons or photons in a porous media sample, require a highly-controlled environment and can be a costly process. To contribute to the development of new methods for characterizing porous media, this paper investigates the feasibility of

using vibroacoustography (VA) as a low-cost and suitable NDT technique for estimating the porosity of rock samples. Additionally, the VA signal can be acquired on the same side of emission (reflection mode) without the necessity of a detector placed on the opposite side of the sample. VA is an ultrasound-based technique that characterizes the mechanical properties of materials [19]–[22]. This technique is based on the nonlinear interaction of two confocal ultrasonic beams at the focus, which generates a low-frequency acoustic response containing information about the mechanical properties of the target [19]–[22]. VA has been widely used in biomedical applications, such as the detection of calcification in arteries [19], [23], characterization of soft tissues [24], [25], detection of kidney stones [26], and evaluation of hip arthroplasty [27]. VA has also been proposed to analyze the bone surface, detect fractures, and evaluate osteoporosis in porous media [28]–[30]. Additionally, VA has been applied to the NDT of metals [31] and the investigation of defects in fiber-reinforced ceramics and electronic chips [32].

The relationship between material porosity and acoustic emission resulting from the interaction of two ultrasound beams was studied by F. G. Mitri [33], who combined finite element model simulations with experimental data to determine the porosity of a chalk sphere. The results in [33] showed that porosity influenced the spectral information of VA. Additionally, M. W. Urban et al. [34] demonstrated that VA signal magnitude and image contrast varied with stiffness and material composition, as a function of the excitation frequency. In this paper, we investigated the feasibility of using multispectral VA to estimate the porosity of rocks. VA signals were acquired from a volumetric region of synthetic ceramics formed by alumina powder sintered with controlled porosity. Then, the VA spectra were analyzed to investigate how the magnitude of acoustic emission was affected by different porosity percentages and to find an optimal spectral band. Finally, the developed experimental protocol was applied in a realistic case involving sandstone rocks analogous to oil reservoir rocks.

2. Materials and methods

2.1. Vibroacoustography experimental setup

The VA experimental setup consisted of a confocal ultrasound transducer with a nominal frequency of 3.4 MHz, which emitted two ultrasound beams of different

frequencies (f_1 and f_2; $\Delta f = |f_1 - f_2|$). The experiments were conducted using the tone burst excitation mode [35], in which the frequency, pulse length, and amplitude of each ultrasound beam were controlled by a two-channel function generator (33522A, Agilent/Keysight, Santa Rosa, California, USA) connected to a power amplifier with a gain of 20 dB produced at our laboratory. The VA signal was acquired using a hydrophone (ITC-6050C, Gavial ITC, Santa Barbara, California, USA) connected to an oscilloscope card (PCI-5122, National Instruments, Austin, Texas, USA). The samples were affixed to a 3D stage for positioning and tracking, which was controlled using a motion card (PCI-7340, National Instruments, Austin, Texas, USA). The emission, acquisition, and tracking parameters were controlled using software programmed in LABVIEW (National Instruments, Austin, Texas, USA).

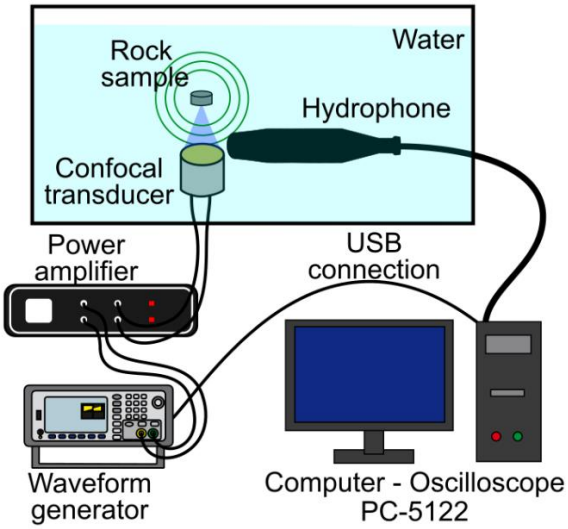

(a)

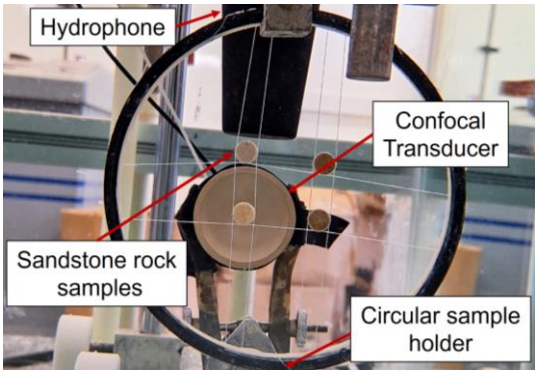

(b)

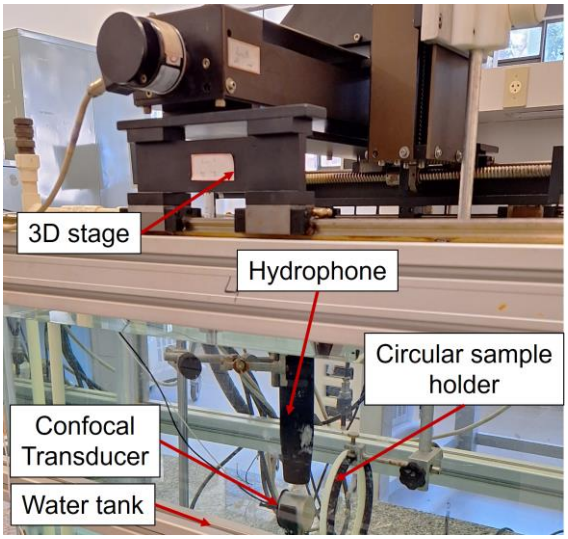

(c)

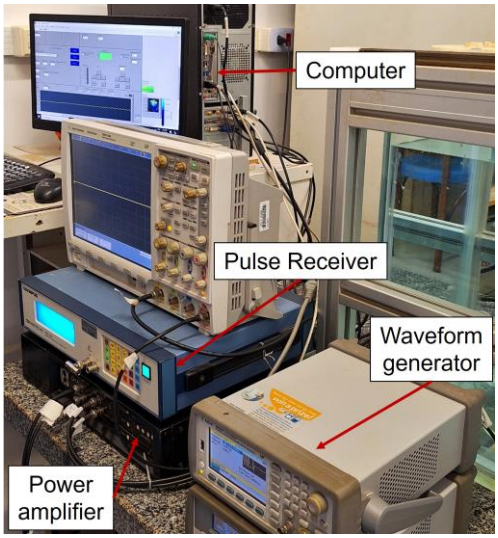

(d)

Figure 1. (a) Illustration of VA experimental setup. The confocal transducer emits ultrasound beams with different frequencies generating a low-frequency acoustic response in rock samples. The vibroacoustic signal was acquired by a hydrophone. (b) Photograph of sandstone rock samples attached to the circular sample holder and aligned to confocal transducer. (c) Photograph of water tank and 3D stage. (d) Photograph of the controller computer, power amplifier, function generator, and pulse-receiver.

The position and alignment of the samples were defined by measuring the distance between the target and the transducer with the pulse/echo technique, using a pulse/receiver system (5800PR, Olympus, Tokyo, Japan). All VA experiments were conducted in a water tank with dimensions of 40 × 55 × 100 cm. Figure 1 depicts the VA experimental setup.

2.2. Vibroacoustography acquisition protocols

The VA acquisition protocols comprised two procedures: VA spectrum and VA images. In the VA spectrum protocol, multispectral VA signals were acquired using Δf ranging from 35 to 85 kHz, with a step of 1 kHz, in a volumetric region of 5 × 5 × 5 mm. The spacing between each acquisition point was 0.5 mm, resulting in an averaged VA signal of 1000 measurements. The measurements were conducted for three volumetric regions centered in different positions on the surface of both synthetic ceramics and sandstone rocks. The root-mean-square (RMS) of the averaged VA signal obtained in the volumetric region for each Δf was calculated to generate the VA spectrum. In the VA image protocol, VA signals were acquired using Δf = 85 kHz, tracking a region of 8.4 × 8.4 mm on the surface of synthetic ceramics and a region of 11 × 11 mm on the surface of sandstone rocks. The spacing between each acquisition point was 0.2 mm.

2.3. Synthetic ceramic samples

The experiments were performed using a series of fifteen cylindrical synthetic ceramic samples (6.34 mm in diameter and 8.0 mm in height) produced by sintering alumina powder (A 1000 SG, Almatis, USA), with an average particle size of 0.6 μm and a surface area of 8.2 m²/g. These samples were manufactured with 5 different proportions (0 – 30 vol%) of naphthalene particles, classified into a sieve system, 38 – 300 μm (ASTM #400 – #50 Mesh/Tyler), used as a pore former. The alumina/naphthalene samples were uniaxially pressed with 100 MPa into an 8 mm metal die. Subsequently, the naphthalene was removed by sublimation at 55°C – 120hs + 60°C – 24h + 80°C – 24h in

a heated chamber before sintering the alumina at 1550°C – 1h. More information about the production of porous ceramics using pore formers is provided by M. N. D'Eurydice *et al.* [36] and R. Del Colle *et al.* [37]. The synthetic ceramic samples were labeled according to their designed porosity, with the nomenclature S_0, S_5, S_{10}, S_{20}, and S_{30} used for synthetic ceramics designed with naphthalene proportions of 0, 5, 10, 20, and 30 vol%, respectively. The resulting porosity percentages of the samples after the sintering process were determined volumetrically (mass divided by the measured external volume) and compared to the theoretical density of alumina (3.95 g/cm3). The resulting porosity percentages are listed in Table 1.

Table 1. The porosity percentages of the synthetic ceramic samples were obtained volumetrically. Fifteen samples with five different porosities were used and divided into three groups (I, II, and III), each group having the same porosity.

Sample	Group I (%)	Group II (%)	Group III (%)	Mean (%)
S_0	6.4	4.0	3.7	5 ± 1
S_5	7.0	6.0	8.0	7 ± 1
S_{10}	10.0	10.0	12.0	11 ± 1
S_{20}	13.0	16.0	16.0	15 ± 2
S_{30}	24.0	22.0	20.0	22 ± 2

The synthetic ceramic samples were affixed to a circular sample holder with a diameter of 15 cm, utilizing a cotton thread with a diameter of 0.1 mm. This arrangement facilitated the acquisition of VA signals from the samples with minimal interference from other structures. Figure 2 depicts the synthetic ceramics affixed to the sample holder.

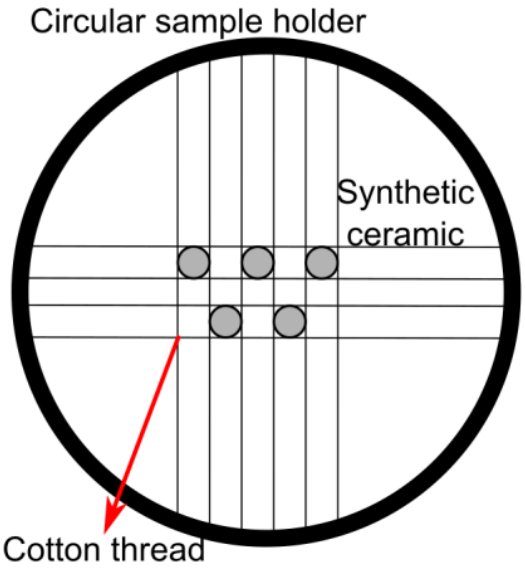

Figure 2. Illustration of the synthetic ceramics attached to a circular sample holder using cotton thread.

Before the experiments, the synthetic ceramic samples were affixed to the sample holder and placed inside a vacuum chamber with a negative pressure of approximately 90 kPa to eliminate air from the pores. The samples were subsequently submerged in water to ensure complete pore intrusion.

2.4. Sandstone rock samples

Eleven sandstone rocks, acquired by *Korurek Industries*, were utilized to evaluate the VA response in a realistic scenario as a function of porosity. E. Lucas-Oliveira *et al.* [16] determined the porosity values, pore size distribution, and permeability of the samples through the application of 3D X-ray microtomography, inert gas pressure, and NMR T_2 distribution. These same samples were previously analyzed by K. E. Washburn et al. [15]. Similar to the synthetic ceramics, the sandstone samples were fastened to a circular sample holder using cotton thread and placed inside a vacuum chamber to fill the pores with water. Table 2 summarizes the porosity percentages in the sandstone rock samples measured using NMR and gas inert pressure.

Table 2. The porosity percentages of the sandstone rock samples were obtained by the NMR and gas inert pressure method [16].

Sandstone sample	Label	NMR Porosity (%)	Gas/He Porosity (%)
Parker	Pk	15.2	14.8
Bandera Gray	BG	17.0	18.1
Berea Sandstone	BS	17.9	19.0
Berea Upper Gray	BUG	18.3	18.6
Berea Sister Gray	BSG	19.6	19.1
Leopard	Lp	19.3	20.2
Kirby	Kb	20.3	20.0
Berea Buff	BB	22.6	24.0
Bentheimer	Bth	23.1	22.6
Bandera Brown	Bbr	24.6	24.1
Boise	Boise	29.0	32.8

3. Results and Discussion

The VA response as a function of porosity was initially examined in the VA spectrum of synthetic ceramics, and subsequently in sandstone rocks. The synthetic ceramics experiments were adopted as the experimental standards, given that the samples were composed of the same material and had identical pore sizes, with the only difference being the fractions of void volume. Because of this characteristic of the synthetic ceramic samples, it is reasonable to assume that the changes in the VA spectrum primarily result from differences in porosity percentages.

In contrast, sandstone rocks are a more realistic case study, where the samples have varying porosity percentages and different compositions and pore size distributions. These properties of the sandstones can affect the VA signal since both the vibration resonance and the nonlinear scattering of ultrasound waves in the focal region rely on several mechanical properties of the material, such as Young's modulus, density, Poisson's ratio, and porosity [22], [33]. Consequently, it is expected that the VA spectrum will convey information about the mechanical properties of the sandstones, including porosity.

3.1. Vibroacoustography of synthetic ceramics

F. G. Mitri [33] compared simulations with experimental data to calculate the porosity of a chalk sphere as an absolute value using the Duckworth-Knudsen equation [38]. To achieve this, mechanical characterization of the chalk sphere was necessary to obtain the density, Young's modulus, and Poisson's ratio. In this investigation, however, only experimental data were utilized to establish a relationship between the porosity and VA response of both synthetic ceramic and rock samples.

The synthetic ceramic samples were manufactured from the same material, with an identical pore size distribution, but differing porosities, thereby enabling changes in the VA response to be attributed to the porosity value. As such, establishing a direct relationship between porosity and VA response could represent an initial step toward developing a protocol for estimating the porosity of rocks.

Figure 3 illustrates the average VA spectra obtained from three groups of synthetic ceramics (I, II, III) with similar porosity percentages, as listed in Table 1. Frequencies ranging from 35 to 85 kHz were utilized for all groups. In the normalized VA spectrum, peak positions and widths are similar to those of the VA responses obtained from a chalk sphere (as presented by F. G. Mitri [33]) and bone samples (as presented by P. M. Agnollitto *et al.* [30]) where found.

In terms of porosity percentages, the VA spectrum in Figure 3 indicates that porosity affects the VA signal amplitude depending on the frequency band. Specifically, the VA signal amplitude increases with increasing porosity within the range of 50 – 60 kHz and 80 – 85 kHz. However, the peak at around 69 kHz does not appear to convey information about porosity since only the synthetic ceramic S_0 magnitude value differed from the other synthetic ceramics.

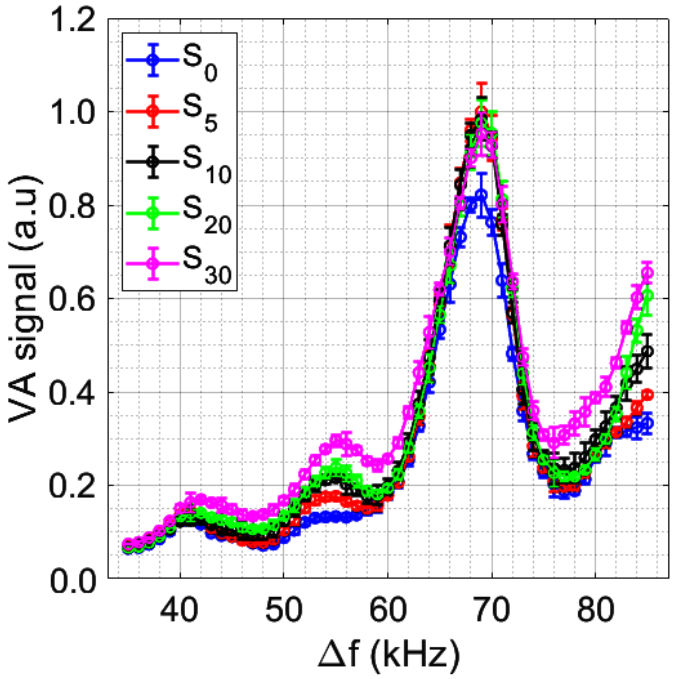

Figure 3. Average VA spectra of synthetic ceramic samples.

The quantitative analysis of the VA spectra of synthetic ceramics was performed by calculating the Pearson correlation coefficient (r) and the slope of the linear fitting between the VA frequency response and rock porosity. A certain frequency range of the VA spectrum was selected within a window with an arbitrary length (kernel), starting at an arbitrary frequency (initial frequency), and the correlation coefficient and slope of the VA signal as a function of porosity were calculated. The initial frequency was then increased by 1.0 kHz to track the entire spectrum. This process was repeated for all possible kernel lengths, ranging from a minimum length of one frequency to a maximum length of 51 frequencies.

Figure 4 displays the correlation coefficient and slope of linear fitting maps for all combinations of kernel length and initial frequency. Some frequency bands of the VA spectra were more sensitive to the porosity of the sample. For instance, the regions of the VA spectrum between 55 – 60 kHz and 82 – 85 kHz displayed high correlation coefficient values. However, the 82 – 85 kHz range exhibited a more pronounced linear slope, indicating that porosity could have a greater impact in this band. The VA response in the 82 – 85 kHz band as a function of porosity is shown in Figure 5.

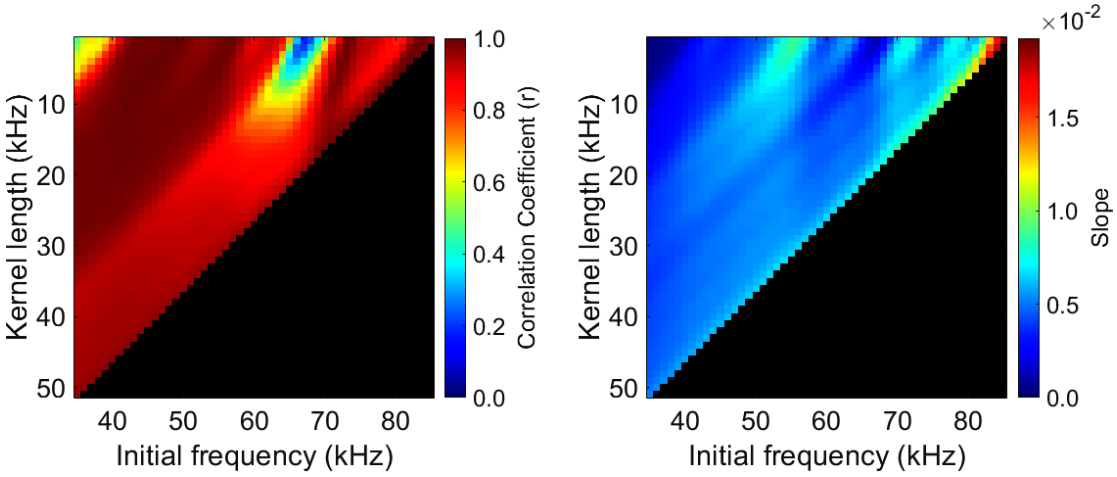

Figure 4. Analysis of VA spectra as a function of kernel length and initial frequency for (a) the correlation coefficient and (b) the slope of the linear fitting of VA signal value as a function of porosity.

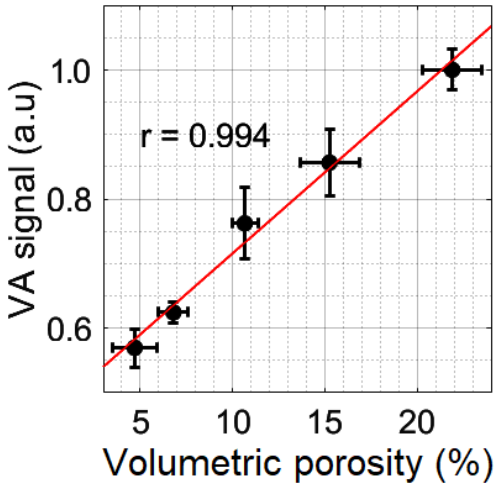

Figure 5. VA response as a function of synthetic ceramic porosity in the 82 – 85 kHz range.

The quantitative analysis of VA spectra indicates that the VA response of synthetic ceramics increased linearly with porosity, primarily for Δf around 85 kHz. Although these results did not estimate the porosity as an absolute value, identifying this linear trend of VA response is an important step in developing a protocol for estimating

material porosity using the VA technique. The subsequent step involved estimating the porosity using the VA spectrum acquired from sandstone rock samples.

3.2. Vibroacoustography spectra of sandstone rock samples

Figure 6 illustrates the VA spectra of sandstone rocks, where for better visualization, the VA spectra of the sandstone rocks are segregated into groups of rocks with similar porosity percentages. Specifically, Figures 6(a), 6(b), and 6(c) exhibit the VA spectra of sandstone rock samples with porosity percentages of 15.2 – 17.9%, 18.3 – 20.3%, and 22.6 – 29.0%, respectively.

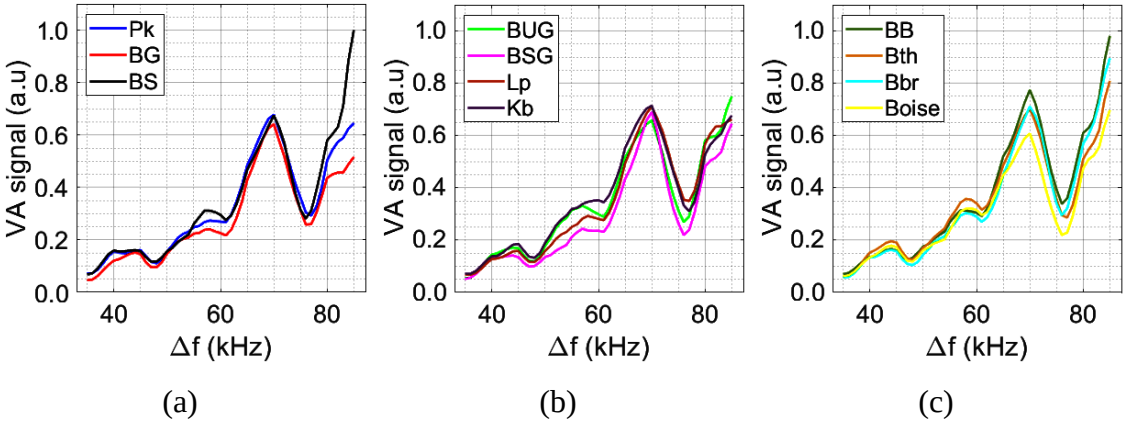

Figure 6. VA spectra of sandstone rock samples with porosity percentages (a) 15.2 – 17.9 %, (b) 18.3 – 20.3 %, and (c) 22.6 – 29.0 %.

The VA spectra of sandstone rocks exhibit similar peak positions and widths to those observed in the synthetic ceramic samples and other studies [30], [33]. Generally, sandstone samples with similar porosities exhibit comparable spectra. In the spectral band from 82 – 85 kHz, where the synthetic ceramics are more sensitive to porosity, the VA response of sandstone rocks appears to maintain the same characteristic of a signal increasing as a function of porosity. However, the Berea Sandstone (BS) sample produces a high VA signal around 85 kHz, even with a porosity percentage of 17.9 % (Figure 6a). On the other hand, the Boise sample, with the highest porosity percentage (29.0%), presents the lowest signal amplitude within the 22.6 – 29.0% porosity group (Figure 6c). It is worth noting that the BS sample exhibits a VA spectrum behavior similar to the VA spectra of the high porosity group (Figure 6c), particularly in regions between 50 – 60 kHz and 80 – 85 kHz. Conversely, the Boise sample has a VA spectrum similar

to that of the high porosity group (Figure 6c), but with a lower VA signal.

To demonstrate these observations quantitatively, the average VA responses of sandstone rocks in the 82 – 85 kHz range are shown in Figure 7.

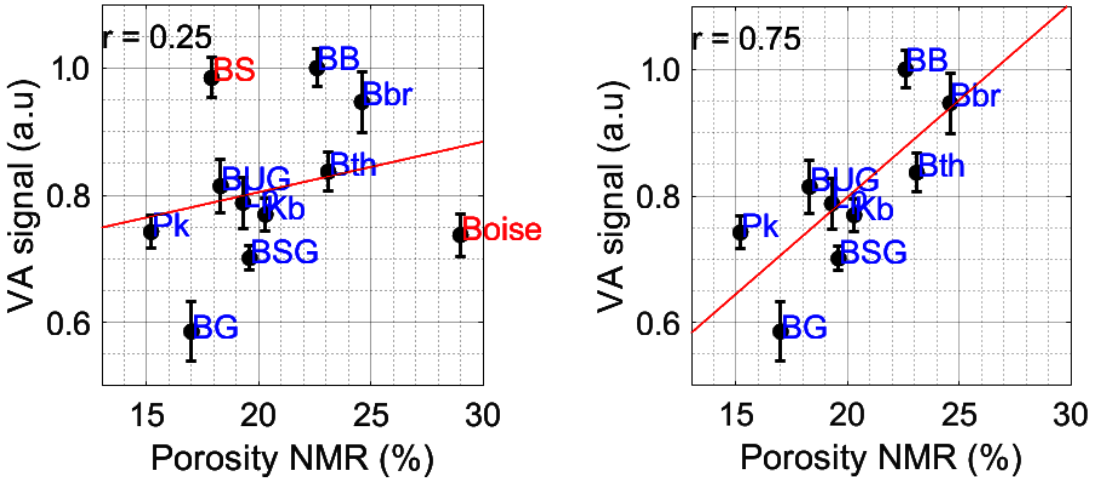

(a) (b)

Figure 7. (a) Average VA signal in the 82 – 85 kHz range as a function of sandstone rock porosity measured by NMR. (b) Average VA signal in the 82 – 85 kHz range as a function of sandstone rock porosity measured by NMR, excluding Berea Sandstone and Boise samples.

The VA response of sandstone rocks, in general, exhibited a linear increasing trend as a function of porosity in the 82 – 85 kHz spectral region (Figure 7a). When excluding the BS and Boise samples from the analysis, the linear trend became more pronounced, and the correlation coefficient increased from r = 0.25 to r = 0.75 (Figure 7b). Despite the deviations observed in the BS and Boise samples, the sandstone rocks demonstrated a signal-increasing trend as a function of porosity that was similar to that observed in synthetic ceramics. This finding suggests that the VA technique has the potential to assess the porosity of rocks, even those with different compositions and pore size distributions. The following section will discuss the potential of VA 2D images to investigate the morphological characteristics of samples with varying porosities.

3.3. Comparison between Vibroacoustography images and Viboacoustography averaged signal

Figure 8 shows the VA images of the surface of synthetic ceramic samples from

group I (see Table 1) acquired using Δf = 85 kHz.

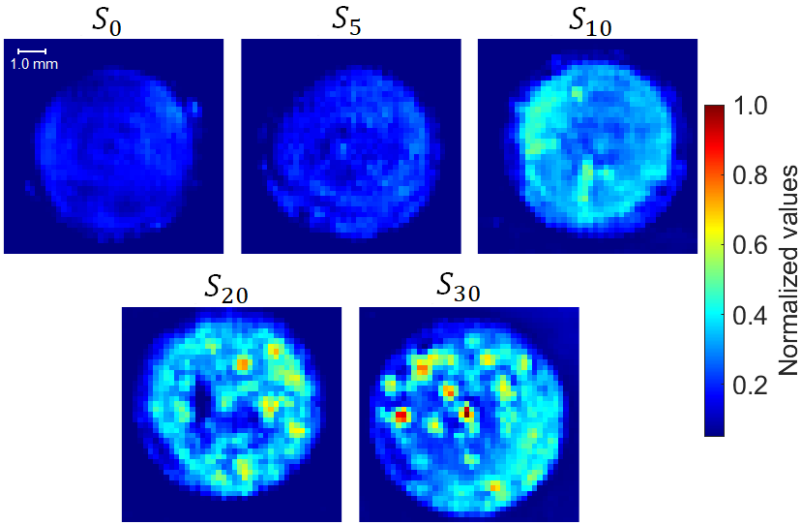

Figure 8. VA image acquired using Δf = 85 kHz for synthetic ceramic samples from group I (see Table 1).

The pixel intensity values of the VA images exhibited a global increase as a function of porosity. An interesting observation was the presence of hot spots, characterized by high VA signals, in the images of synthetic ceramics S_{10}, S_{20}, and S_{30}, whereas the images of synthetic ceramics S_0 and S_5 appeared more homogeneous. The quantitative analysis involved calculating the average pixel intensity values for each VA image of all synthetic ceramics, as shown in Table 1. Figure 9 illustrates the average VA intensity values for the images obtained with the synthetic ceramics.

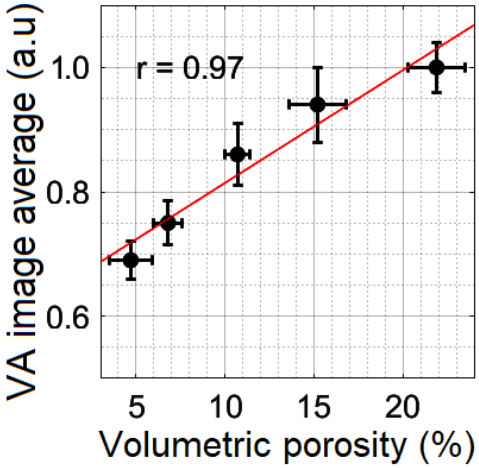

Figure 9. Average VA intensity values in the delimited region of synthetic ceramics of groups I, II, and III.

291

292 The average VA intensity in the images also showed a linear increasing tendency
293 as a function of porosity for the synthetic ceramics. Figure 10 displays the VA images
294 obtained with the sandstone rocks.

295

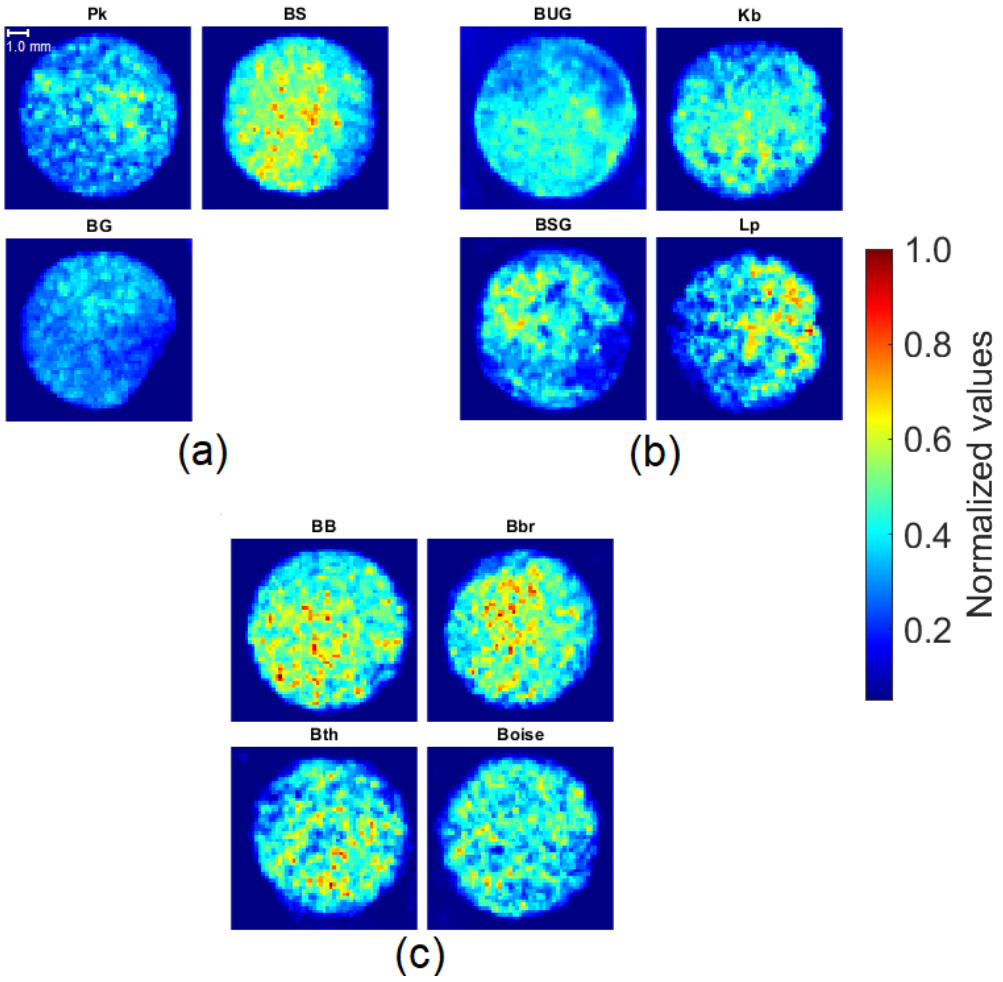

296

297 Figure 10. The VA images were acquired using Δf = 85 kHz for sandstone rock samples with
298 porosity percentages (a) 15.2 – 17.9 %, (b) 18.3 – 20.3 %, and (c) 22.6 – 29.0 %.

299

300 Similar to the VA images obtained with synthetic ceramics, the VA images
301 acquired from sandstone rocks exhibited a global increase in intensity as a function of
302 porosity (refer to Figure 11). Additionally, hot spots were observed in samples with higher
303 porosity in the case of sandstone rocks.

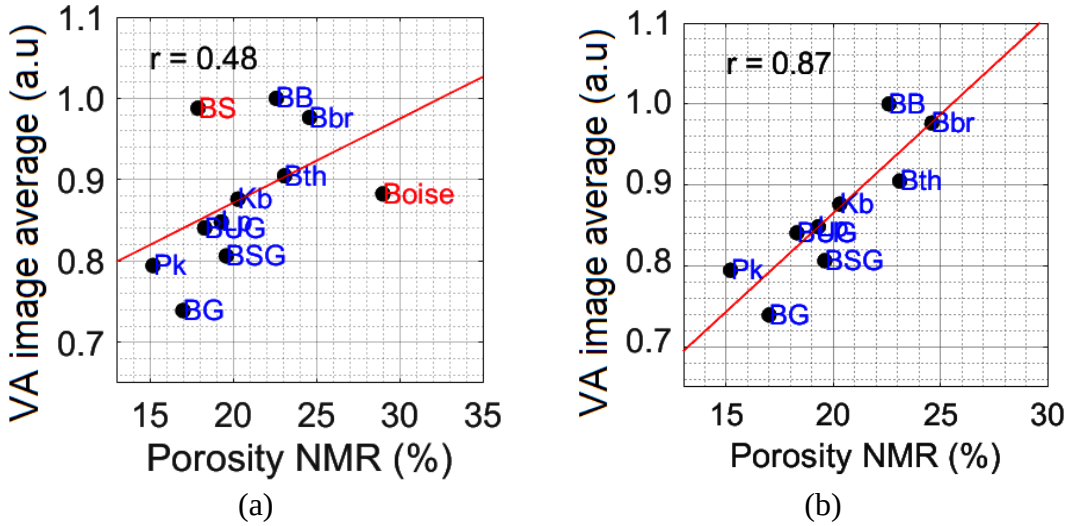

Figure 11. Average pixel intensity in the delimited region of (a) all samples of sandstone rocks and (b) excluding BS and Boise samples.

The analysis of the VA images produced similar results to those found for the VA spectra acquired in a volumetric region for both synthetic ceramics and sandstone rocks. As shown in Figure 10, the average intensity of pixel values, as well as the number of hot spots, increased with the porosity of the samples. However, the BS sample exhibited a large number of hot spots even with a porosity value of 17.9%, resulting in an image texture that differed from the group with porosities of 15.2 – 17.9% and was similar to the group with porosities of 22.6 – 29.0%. For the Boise sample, the texture of the image was similar to the group with porosities of 22.6 – 29.0%, but the intensity of pixels was lower, reducing the image average intensity. This characteristic in the image texture is analogous to the behavior observed for the VA spectrum for the BS and Boise samples presented in the previous section.

The results suggest that the VA technique has the potential to be a valuable tool for directly estimating material porosity. The comparison of the VA technique with the NMR estimation of porosity is important to evaluate both the feasibility and limitations of the VA technique. The manufacturing of synthetic ceramics plays an important role in this context, as it can produce samples with controlled porosity and pore sizes, made from alumina, which is a universal ceramic [39]. In the NMR technique, the fluid dynamics inside the pores can estimate porosity, pore radius distributions, and permeability, which are calibrated using synthetic alumina ceramics [36] due to the low signal from the structure of the pores, with the major signal coming from the fluid. On the other hand, the

VA signal comes from the structure, and synthetic alumina ceramic is a good calibration sample due to its uniform pore sizes and being composed of purely alumina. In this case, both techniques converge to good results, as demonstrated in Fig. 5 for VA and in [36] for NMR.

In the realistic case of sandstone rocks, the composition of rocks is not uniform and could change the VA signal beyond purely porosity, posing a challenge to the proposed technique. Here, the NMR estimation of porosity was used as a standard due to its good accuracy (Table 2), and the VA technique presented a lower correlation coefficient with porosity in comparison with the value observed for synthetic ceramics. Moreover, an important concern in the results found in this work is the inverse relationship of VA signal amplitude with porosity that describes by [24], [29] for bone and ceramic samples. The hot spots presented in Figs. 8 and 10 contribute to the increase of VA signal, but they need to be analyzed in a depth to clarify their relation with the porosity of sample, pore size distribution and the complex connectivity of the pores.

To fully understand the physical mechanisms behind the hot spots observed in VA images and the increasing trend of averaged VA signal with porosity, a complete mechanical and morphological characterization of sandstone rocks is necessary. This will allow for a comparison of experimental data with mathematical models and computational simulations. Additionally, the production of artificial rocks with different mechanical properties (such as varying elastic modulus) and pore size distributions could help evaluate the contribution of each parameter individually and develop a robust multivariable model for porosity estimation using the VA technique.

While these results provide promising initial evidence of the feasibility of direct porosity measurement using the VA technique, further studies are required to develop instrumentation and protocols for measuring porosity in materials. Additionally, the nondestructive, noncontact, and reflection mode nature of the VA technique [21], [32], [33] makes it versatile for performing NDT of porous materials in an industrial context without requiring complex and high-cost equipment.

4. Conclusion

The objective of this study was to investigate the potential of the multifrequency VA technique in estimating the porosity of rocks. This technique is sensitive to the porosity and stiffness of samples, as previously demonstrated by F. G. Mitri and M. W.

Urban *et al*. We evaluated the VA response in synthetic ceramics and sandstone rocks to establish its correlation with the porosity of rocks. The results indicated a linear increase in the VA signal amplitude as a function of porosity for synthetic ceramics with controlled porosity values, signifying the sensitivity of the technique to the porosity of the material. Similarly, we found a linear increase in the VA signal with porosity for nine out of eleven sandstone rock samples.

Based on these findings, the VA technique has great potential as a nondestructive testing method for estimating the porosity of rock samples in an industrial context. It is low-cost, operates in reflection mode, and is suitable for nondestructive testing, making it a promising alternative to more intricate and costly methods. This study contributes to the development of new methods for characterizing porous media, particularly in the context of nondestructive testing techniques. The results of this study could have relevance for various applications, including industrial processes and biomedicine, where the porosity of materials is a critical parameter.

5. Declaration of competing interest

The authors declare no conflict of interest.

6. CRediT authorship contribution statement

João H. Uliana: Conceptualization, Investigation, Software, Validation, Methodology, Formal analysis, Data curation, Writing - original draft. **Guilherme A. Bráz**: Conceptualization, Investigation, Methodology, Software, Writing review & editing. **Éverton L. Oliveira:** Conceptualization, Investigation, Methodology, Writing review & editing. **Arthur G. Araujo-Ferreira**: Conceptualization, Investigation, Methodology, Writing review & editing. **Mateus M. Morais**: Conceptualization, Investigation, Methodology, Formal analysis, Data curation, Writing review & editing. **Willian A. Trevizan**: Methodology, Resources, Investigation, Writing review & editing. **Carlos A. Fortulan**: Supervision, Conceptualization, Resources, Writing - review & editing. **Tito J. Bonagamba**: Supervision, Conceptualization, Project administration, Resources, Funding acquisition,Writing - review & editing. **Theo Z. Pavan**: Supervision, Conceptualization, Methodology, Formal analysis, Writing - original draft, Writing - review & editing. **Antonio A. O. Carneiro**: Supervision, Conceptualization,

Investigation, Methodology, Formal analysis, Data curation, Writing - original draft, Writing - review & editing.

7. Acknowledgments

Authors acknowledge the support of the following Institutions: Universidade de São Paulo (USP), Brazil; Centro de Pesquisa e Desenvolvimento Leopoldo Américo Miguez de Mello (Cenpes), Brazil, (CENPES/Petrobras, 2020/00010-0). T. J. Bonagamba acknowledges National Council for Scientific and Technological Development, Brazil (CNPq, 308076/2018-4) and São Paulo Research Foundation, Brazil (FAPESP, 2009/54880-6). A. A. O. Carneiro acknowledges São Paulo Research Foundation, Brazil (FAPESP, 2018/16939-8), National Council for Scientific and Technological Development, Brazil (CNPq, 311224/2021-0).

8. References

[1] L. Espinal, "Porosity and Its Measurement," *Charact. Mater.*, 2012, doi: 10.1002/0471266965.com129.

[2] G. Han and M. B. Dusseault, "Description of fluid flow around a wellbore with stress-dependent porosity and permeability," *J. Pet. Sci. Eng.*, vol. 40, no. 1–2, pp. 1–16, 2003, doi: 10.1016/S0920-4105(03)00047-0.

[3] M. Lawrence and Y. Jiang, "Porosity: Pore Size Distribution, Micro-structure," in *Bio-aggregates Based Building Materials*, Vol. 23., F. Amziane, S., Collet, Ed., Dordrecht: Springer, 2017, pp. 39–71. doi: 10.1007/978-94-024-1031-0_2.

[4] M. L. McKelvie and S. B. Palmer, "The interaction of ultrasound with cancellous bone," *Phys. Med. Biol.*, vol. 36, no. 10, pp. 1331–1340, 1991, doi: 10.1088/0031-9155/36/10/003.

[5] S. Bose, M. Roy, and A. Bandyopadhyay, "Recent advances in bone tissue engineering scaffolds," *Trends Biotechnol.*, vol. 30, no. 10, pp. 546–554, 2012, doi: 10.1016/j.tibtech.2012.07.005.

[6] J. Compston *et al.*, "UK clinical guideline for the prevention and treatment of osteoporosis," *Arch. Osteoporos.*, vol. 12, no. 1, 2017, doi: 10.1007/s11657-017-0324-5.

[7] U. Tarantino *et al., Clinical guidelines for the prevention and treatment of osteoporosis: summary statements and recommendations from the Italian Society for Orthopaedics and Traumatology*, vol. 18, no. s1. Springer International Publishing, 2017. doi: 10.1007/s10195-017-0474-7.

[8] D. A. Jerram and M. D. Higgins, "3D analysis of rock textures: Quantifying igneous microstructures," *Elements*, vol. 3, no. 4, pp. 239–245, 2007, doi: 10.2113/gselements.3.4.239.

[9] T. J. Haire and C. M. Langton, "Biot theory: A review of its application to ultrasound propagation through cancellous bone," *Bone*, vol. 24, no. 4, pp. 291–295, 1999, doi: 10.1016/S8756-3282(99)00011-3.

[10] Z. E. A. Fellah, M. Sadouki, M. Fellah, F. G. Mitri, E. Ogam, and C. Depollier, "Simultaneous determination of porosity, tortuosity, viscous and thermal characteristic lengths of rigid porous materials," *J. Appl. Phys.*, vol. 114, no. 20, pp. 1–6, 2013, doi: 10.1063/1.4833546.

[11] R. Bai, A. Tinel, A. Alem, H. Franklin, and H. Wang, "Estimating frame bulk and shear moduli of two double porosity layers by ultrasound transmission," *Ultrasonics*, vol. 70, pp. 211–220, 2016, doi: 10.1016/j.ultras.2016.05.004.

[12] C. Liu, Aqib, Z. Wang, and Y. Wang, "Experimental research on the acoustic transmission characteristics of refractory materials," *J. Brazilian Soc. Mech. Sci. Eng.*, vol. 42, no. 6, pp. 1–10, 2020, doi: 10.1007/s40430-020-02409-z.

[13] O. Bahrami Khameslouie, M. H. Soorgee, E. Ghafarallahi, and S. E. Moussavi Torshizi,

"Comparison between elastic and porous elastic material models for sediment acoustical behavior in an aluminum-sediment double layer," *J. Brazilian Soc. Mech. Sci. Eng.*, vol. 43, no. 5, pp. 1–11, 2021, doi: 10.1007/s40430-021-02988-5.

[14] S. Garia, A. K. Pal, K. Ravi, and A. M. Nair, "A multivariate statistical approach in correlating the acoustic properties with petrophysics and mineralogy on sandstones," *Geophys. J. Int.*, vol. 230, no. 1, pp. 160–178, 2022, doi: 10.1093/gji/ggac061.

[15] K. E. Washburn, M. Sandor, and Y. Cheng, "Evaluation of sandstone surface relaxivity using laser-induced breakdown spectroscopy," *J. Magn. Reson.*, vol. 275, pp. 80–89, 2017, doi: 10.1016/j.jmr.2016.12.004.

[16] E. Lucas-Oliveira, A. G. Araujo-Ferreira, W. A. Trevizan, B. C. Coutinho dos Santos, and T. J. Bonagamba, "Sandstone surface relaxivity determined by NMR T2 distribution and digital rock simulation for permeability evaluation," *J. Pet. Sci. Eng.*, vol. 193, no. April, p. 107400, 2020, doi: 10.1016/j.petrol.2020.107400.

[17] D. Wildenschild, J. W. Hopmans, C. M. P. Vaz, M. L. Rivers, D. Rikard, and B. S. B. Christensen, "Using X-ray computed tomography in hydrology: systems, resolutions, and limitations.," *J. Hydrol.*, vol. 267, pp. 285–297, 2002, doi: https://doi.org/10.1016/S0022-1694(02)00157-9.

[18] M. K. Lim and H. Cao, "Combining multiple NDT methods to improve testing effectiveness," *Constr. Build. Mater.*, vol. 38, pp. 1310–1315, 2013, doi: 10.1016/j.conbuildmat.2011.01.011.

[19] M. Fatemi and J. F. Greenleaf, "Ultrasound-stimulated vibro-acoustic spectrography," *Science (80-.).*, vol. 280, no. 5360, pp. 82–85, 1998, doi: 10.1126/science.280.5360.82.

[20] M. Fatemi and J. F. Greenleaf, "Vibro-acoustography: An imaging modality based on ultrasound-stimulated acoustic emission," *Proc. Natl. Acad. Sci. U. S. A.*, vol. 96, no. 12, pp. 6603–6608, 1999, doi: 10.1073/pnas.96.12.6603.

[21] M. Fatemi and J. F. Greenleaf, "Application of radiation force in noncontact measurement of the elastic parameters," *Ultrason. Imaging*, vol. 21, no. 2, pp. 147–154, 1999, doi: 10.1177/016173469902100205.

[22] G. T. Silva and F. G. Mitri, "Difference-frequency generation in vibro-acoustography," *Phys. Med. Biol.*, vol. 56, no. 18, pp. 5985–5993, 2011, doi: 10.1088/0031-9155/56/18/013.

[23] C. Pislaru *et al.*, "In vivo vibroacoustography of large peripheral arteries," *Invest. Radiol.*, vol. 43, no. 4, pp. 243–252, 2008, doi: 10.1097/RLI.0b013e31816085fc.

[24] S. Callé, J. P. Remeniéras, F. Patat, and O. B. Matar, "Application of Vibro-Acoustography to Tissue Elasticity Imaging," *Acta Acust.*, vol. 89, no. 6, pp. 936–941, 2003.

[25] H. Yuan, B. B. Guzina, S. Chen, R. Kinnick, and M. Fatemi, "Application of topological sensitivity toward soft-tissue characterization from vibroacoustography measurements," *J. Comput. Nonlinear Dyn.*, vol. 8, no. 3, pp. 1–6, 2013, doi: 10.1115/1.4023738.

[26] F. G. Mitri and R. R. Kinnick, "Vibroacoustography imaging of kidney stones in vitro," *IEEE Trans. Biomed. Eng.*, vol. 59, no. 1, pp. 248–254, 2012, doi: 10.1109/TBME.2011.2171341.

[27] H. A. S. Kamimura, L. Wang, A. A. O. Carneiro, R. R. Kinnick, K. N. An, and M. Fatemi, "Vibroacoustography for the assessment of total hip arthroplasty," *Clinics*, vol. 68, no. 4, pp. 463–468, 2013, doi: 10.6061/clinics/2013(04)05.

[28] F. G. Mitri, R. R. Kinnick, J. F. Greenleaf, and M. Fatemi, "Bone Imaging Using Tone-Burst Vibro-acoustography and Pulse-Echo Ultrasound : A Qualitative Comparative Study," *Curr. Med. Imaging Rev.*, vol. 7, no. 4, pp. 350–359, 2011, doi: 10.2174/157340511798038648.

[29] M. H. Nogueira-Barbosa, H. A. S. Kamimura, G. Braz, P. M. Agnollitto, and A. A. O. Carneiro, "Preliminary results of vibro-acoustography evaluation of bone surface and bone fracture," *Quant. Imaging Med. Surg.*, vol. 7, no. 5, pp. 549–554, 2017, doi: 10.21037/qims.2017.09.05.

[30] P. M. Agnollitto, G. De Araújo Braz, A. L. Spirlandeli, F. J. A. De Paula, A. A. O. Carneiro, and M. H. Nogueira-Barbosa, "Ex vivo vibro-acoustography characterization of osteoporosis in an experimental mice model," *Quant. Imaging Med. Surg.*, vol. 11, no. 2, pp. 586–596, 2021, doi: 10.21037/QIMS-20-610.

[31] B. S. Marció, A. A. Seibert, G. de A. Braz, A. A. O. Carneiro, and R. C. C. Flesch, "Nondestructive inspection of metal specimen using tone-burst vibro-acoustography," *Ultrasonics*, vol. 111, no. November 2020, 2021, doi: 10.1016/j.ultras.2020.106339.

[32] F. G. Mitri and M. Fatemi, "Improved vibroacoustography imaging for nondestructive inspection of materials," *J. Appl. Phys.*, vol. 98, no. 11, 2005, doi: 10.1063/1.2130515.

[33] F. G. Mitri, "Inverse determination of porosity from object's resonances," *J. Appl. Phys.*, vol. 96, no. 10, pp. 5866–5869, 2004, doi: 10.1063/1.1805716.

[34] M. W. Urban, G. T. Silva, M. Fatemi, and J. F. Greenleaf, "Multifrequency vibro-acoustography," *IEEE Trans. Med. Imaging*, vol. 25, no. 10, pp. 1284–1295, 2006, doi: 10.1109/TMI.2006.882142.

[35] F. G. Mitri, J. F. Greenleaf, and M. Fatemi, "Comparison of continuous-wave (CW) and tone-burst (TB) excitation modes in vibro-acoustography: Application for the non-destructive imaging of flaws," *Appl. Acoust.*, vol. 70, no. 2, pp. 333–336, 2009, doi: 10.1016/j.apacoust.2008.03.005.

[36] M. N. D'Eurydice, E. T. Montrazi, C. A. Fortulan, and T. J. Bonagamba, "T2-Filtered T2-T2 Exchange NMR," *J. Chem. Phys.*, vol. 144, no. 20, 2016, doi: 10.1063/1.4951712.

[37] R. Del Colle, C. A. Fortulan, and S. R. Fontes, "Manufacture and characterization of ultra and microfiltration ceramic membranes by isostatic pressing," *Ceram. Int.*, vol. 37, no. 4, pp. 1161–1168, 2011, doi: 10.1016/j.ceramint.2010.11.039.

[38] R. W. Rice, *Treatise on Materials Science and Technology*, 11th ed. New York: ACADEMIC PRESS INC., 1977.

[39] A. Margarido, B. M. Purquerio, C. R. Foschini, and C. A. Fortulan, "Influence of the green-machining parameters on the mechanical properties of alumina rods," *Int. J. Adv. Manuf. Technol.*, vol. 88, no. 9–12, pp. 3475–3484, 2017, doi: 10.1007/s00170-016-9081-7.